n-Type Conjugated Dendrimers: Convergent Synthesis, Photophysics, Electroluminescence, and Use as Electron-Transport Materials for Light-Emitting Diodes

Tae Woo Kwon,† Maksudul M. Alam, and Samson A. Jenekhe*

Departments of Chemical Engineering and Chemistry, University of Washington, Seattle, Washington 98195-1750

Received March 29, 2004. Revised Manuscript Received April 19, 2004

Three new electron-acceptor and light-emitting conjugated dendrimers, [G1-4Q], [G1-6Q], and [G2-12Q], based on a benzene core, poly(phenylenevinylene) dendrons, and diphenylquinoline peripheral groups have been synthesized, characterized, and used as emissive and electron-transport materials in efficient light-emitting diodes. All three dendrimers emit blue light (λ_{max} = 414 nm) in solution with high fluorescence quantum yields in the 0.69−0.87 range and fluorescence lifetimes of 1.4−1.6 ns. In thin films the dendrimers emit yellow light with poor fluorescence efficiency, suggesting aggregation and excimer formation in the solid state. The dendrimers showed quasi-reversible electrochemical reduction with a formal potential of −2.0 V (vs SCE) and derived LUMO levels of 2.5−2.6 eV, implying that injected electrons are localized in the periphery of the dendrimers. As the emissive materials in light-emitting diodes, the dendrimers showed yellow electroluminescence the brightness and efficiency of which increased with generation and number of electron-acceptor peripheral groups. The performance of bilayer light-emitting diodes using the dendrimers as the electron-transport layers and poly(2-methoxy-5-(2′-ethyl-hexyloxy)-1,4-phenylene vinylene) as the emissive layer increased with generation and number of electron-acceptor peripheral groups, reaching a maximum external efficiency of 5.0%, a power efficiency of 1.3 lm/W, and a brightness of up to 2000 cd/m^2 in ambient air using aluminum cathode. These results demonstrate that electron-acceptor and electron-transport dendrimers can be created by functionalization of the dendrimer periphery. The new dendrimers are promising n-type semiconductors for organic electronic and optoelectronic devices.

Introduction

Electroactive and light-emitting dendrimers are of current interest for developing efficient electroluminescent devices for displays and lighting and other photonic devices.[1−10] Compared to well-known conjugated linear chain polymers, the unusual electronic and photophysical properties of π-conjugated dendrimers, for example intramolecular energy transfer in multichromophoric systems,[7] exciton and charge localization phenomena,[3,6,7] and generation-dependent charge carrier mobility,[6] are also of broad fundamental interest. As emissive materials for light-emitting diodes (LEDs), the dendritic topology of dendrimers is expected to reduce or eliminate strong intermolecular interactions and aggregation

* To whom correspondence should be addressed. E-mail: jenekhe@u.washington.edu.

† Permanent address: Department of Chemistry, Kyungsung University, Busan 608-736, Korea.

(1) (a) Halim, M.; Pillow, J. N. G.; Samuel, I. D. W.; Burn, P. L. *Adv. Mater.* **1999**, *11*, 371−374. (b) Ma, D.; Lupton, J. M.; Samuel, I. D. W.; Lo, S.-C.; Burn, P. L. *Appl. Phys. Lett*. **2002**, *81*, 2285−2287. (c) Ma, D.; Lupton, J. M.; Beavington, R.; Burn, P. L.; Samuel, I. D. W. *Adv. Funct. Mater.* **2002**, *12*, 507−511. (d) Anthopoulos, T. D.; Markham, J. P. J.; Namdas, E. B.; Samuel, I. D. W.; Lo, S.-C.; Burn, P. L. *Appl. Phys. Lett*. **2003**, *82*, 4824−4826.

(2) (a) Freeman, A. W.; Koene, S. C.; Malenfant, P. R. L.; Thompson, M. E.; Fréchet, J. M. J. *J. Am. Chem. Soc*. **2000**, *122*, 12385−12386. (b) Furuta, P.; Brooks, J.; Thompson, M. E.; Fréchet, J. M. J. *J. Am. Chem. Soc*. **2003**, *125*, 13165−13172. (c) Adronov, A.; Fréchet, J. M. J. *Chem. Commun.* **2000**, *18*, 1701−1710. (d) Grayson, S. M.; Fréchet, J. M. J. *Chem. Rev*. **2001**, *101*, 3819−3867.

(3) Wang, P.-W.; Liu, Y.-J.; Devadoss, C.; Bharathi, P.; Moore, J. S. *Adv. Mater*. **1996**, *8*, 237−241.

(4) (a) Setayesh, S.; Grimsdale, A. C.; Weil, T.; Enkelmann, V.; Müllen, K.; Meghdadi, F.; List, E. J. W.; Leising, G. *J. Am. Chem. Soc*. **2001**, *123*, 946−953. (b) Lor, M.; Thielemans, J.; Viaene, L.; Cotlet, M.; Hofkens, J.; Weil, T.; Hampel, C.; Mullen, K.; Verhoeven, J. W.; Auweraer, M. V. D.; Schryver, F. C. D. *J. Am. Chem. Soc*. **2002**, *124*, 9918−9925. (c) Pogantsch, A.; Wenzl, F. P.; List, E. J. W.; Leising, G.; Grimsdale, A. C.; Müllen, K. *Adv. Mater*. **2002**, *14*, 1061−1064.

(5) (a) Satoh, N.; Cho, J.-S.; Higuchi, M.; Yamamoto, K. *J. Am. Chem. Soc*. **2003**, *125*, 8104−8105. (b) Kuwabara, Y.; Ogawa, H.; Inada, H.; Noma, N.; Shirota, Y. *Adv. Mater*. **1994**, *6*, 677−679. (c) Tao, X. T.; Zhang, Y. D.; Wada, T.; Sasabe, H.; Suzuki, H.; Watanabe, T.; Miyata, S. *Adv. Mater*. **1998**, *10*, 226−230. (d) Thelakkat, M. *Macromol. Mater. Eng.* **2002**, *287*, 442−461. (e) Sakamoto, Y.; Suzuki, T.; Miura, A.; Fujikawa, H.; Tokito, S.; Taga, Y. *J. Am. Chem. Soc*. **2000**, *122*, 1832−1833. (f) Xia, C. J.; Fan, X. W.; Locklin, J.; Advincula, R. C. *Org. Lett*. **2002**, *4*, 2067−2070.

(6) (a) Markham, J. P. J.; Anthopoulos, T. D.; Samuel, I. D. W.; Richards, G. J.; Burn, P. L.; Im, C.; Bässler, H. *Appl. Phys. Lett*. **2002**, *81*, 3266−3268. (b) Lupton, J. M.; Samuel, I. D. W.; Beavington, R.; Burn, P. L.; Bassler, H. *Adv. Mater*. **2001**, *13*, 258−261. (c) Lupton, J. M.; Samuel, I. D. W.; Beavington, R.; Frampton, M. J.; Burn, P. L.; Bassler, H. *Phys. Rev. B* **2001**, *63*, 155206.

(7) (a) Devadoss, C.; Bharathi, P.; Moore, J. S. *J. Am. Chem. Soc*. **1996**, *118*, 9635−9644. (b) Kopelman, R.; Shortreed, M.; Shi, Z.-Y.; Tan, W.; Xu, Z.; Moore, J. S.; Bar-Haim, A.; Klafter, J. *Phys. Rev. Lett*. **1997**, *78*, 1239−1242. (c) Lupton, J. M.; Samuel, I. D. W.; Burn, P. L.; Mukamel, S. *J. Chem. Phys*. **2002**, *116*, 455−459. (d) Ranasinghe, M. I.; Varnavski, O. P.; Pawlas, J.; Hauck, S. I.; Louie, J.; Hartwig, J. F.; Goodson, T. *J. Am. Chem. Soc*. **2002**, *124*, 6520−6521. (e) Wang, Y.; Ranasinghe, M. I.; Goodson, T. *J. Am. Chem. Soc*. **2003**, *125*, 9562−9563.

10.1021/cm0494711 CCC: $27.50
Published on Web 06/05/2004

Chart 1. Structures of n-Type Conjugated Dendrimers 1−3

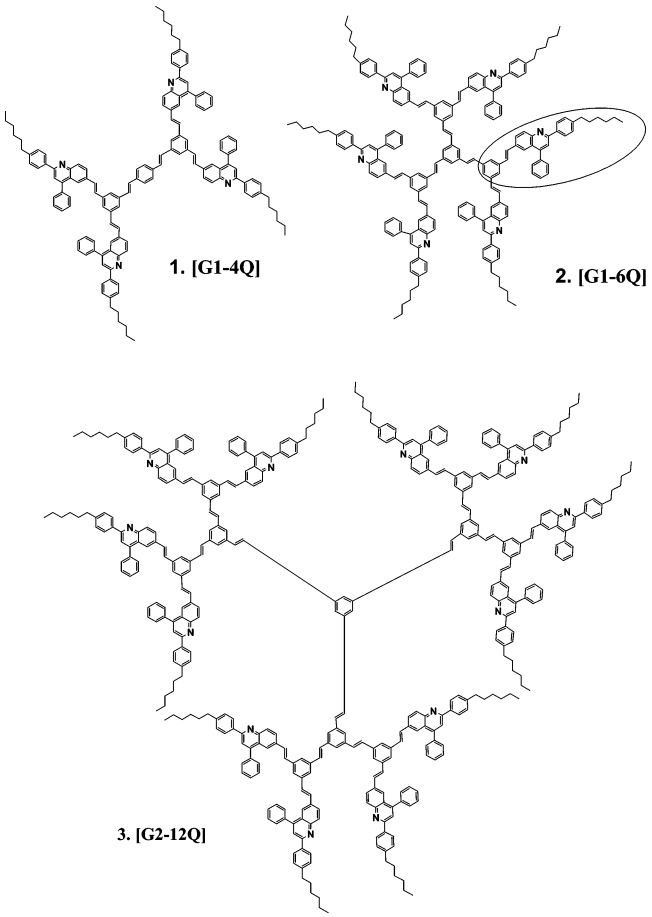

that often lead to excimer formation and reduced emission quantum yields in linear chain conjugated polymers.[1−3] The dendrimer generation was recently demonstrated as an effective approach to controlling the *hole* mobility in organic LEDs.[6] However, only p-type (electron-donor or hole-transport) conjugated dendrimers have been extensively investigated to date.[1−10] n-Type (electron-acceptor) conjugated dendrimers capable of electron transport and light emission are also needed for fundamental studies and for applications in organic LEDs but only a few examples are known.[10]

We report herein the convergent synthesis, the electrochemical and photophysical properties, and the electroluminescence of n-type conjugated dendrimers, [G1-4Q], [G1-6Q], and [G2-12Q] (Chart 1), and their use as electron-transport materials in fabricating bright and efficient organic LEDs. These generation-one and -two dendrimers have poly(phenylenevinylene) dendrons and electron-acceptor diphenyquinoline groups in the periphery. Our prior extensive studies have shown that 4-phenylquinoline[11] and 4-alkylquinoline[12] are excellent building blocks for the design of electron-acceptor (n-type) conjugated linear-chain polymers and molecules with useful electroluminescence,[12−14] electron transport,[13,14] electrochemiluminescence (ECL),[15] nonlinear optical,[16] and other electronic properties. We thus expect these new conjugated dendrimers to similarly have interesting, and perhaps novel, electronic and photonic properties.

The results of prior studies of electroactive and electroluminescent dendrimers suggest a strong dependence of charge transport properties on the dendrimer structure.[6] Studies of dendrimers with hole-transport cores, such as triarylamines, have shown that the carrier mobility decreased by 2 orders of magnitude as the size increased from generation zero to three.[6] This result was explained by the fact that increase in generation, and thus dendron size, increased the intermolecular distance between the hole-transport cores.[6] However, electron-rich triarylamine groups capable of redox activity and hole transport are also commonly placed in the periphery of the dendrimer, leading to effective hole trapping and transport in organic LEDs.[2,3,5] Nonconjugated poly(amidoamine) dendrimers with chemically reduced diimide groups in the periphery were found to give rise to electrically n-type conducting materials with humidit-dependent dc conductivities as high as 10^{-3} to 18 S/cm.[17] The high conductivity was rationalized in terms of intermolecular π-stacking of the peripheral diimide radical anions of adjacent dendrimer molecules.[17] The proposed dendrimers in Chart 1 represent the strategy of placing electron-accepting and light-emitting groups in the periphery of poly(phenylenevinylene) dendrons. As found in linear small molecules,[15] each diphenylquinoline (Q) moiety in each dendrimer could potentially accept an electron. The 4-, 6-, and 12-electron-accepting sites in the dendrimers are shown schematically in Chart 2.

Results and Discussion

Synthesis and Characterization. As a key intermediate in the synthesis of [G1-4Q] (**1**), [G1-6Q] (**2**), and [G2-12Q] (**3**) dendrimers, we designed and synthesized the [G1]-CHO dendron (**4**) containing the diphenylquinoline moieties (Chart 3). Aldehyde-functionalized dendron was used to build up the higher generation via the Horner−Wadsworth−Emmons coupling reaction.[18] Vi-

(8) (a) Hahn, U.; Gorka, M.; Vogtle, F.; Vicinelli, V.; Ceroni, P.; Maestri, M.; Balzani, V. *Angew. Chem., Int. Ed*. **2002**, *41*, 3595−3598. (b) Kwok, C. C.; Wong, M. S. *Macromolecules* **2001**, *34,* 6821−6830.

(9) (a) Chasse, T. L.; Sachdeva, R.; Li, C.; Li, Z. M.; Petrie, R. J.; Gorman, C. B. *J. Am. Chem. Soc.* **2003**, *125*, 8250−8254. (b) Crooks, R. M.; Zhao, M. Q.; Sun, L.; Chechik, V. Yeung, L. K. *Acc. Chem. Res*. **2001**, *34*, 181−190.

(10) (a) Sakamoto, Y.; Suzuki, T.; Miura, A.; Fujikawa, H.; Tokito, S.; Taga, Y. *J. Am. Chem. Soc.* **2000**, *122*, 1832−1833. (b) Bettenhausen, J.; Greczmiel, M.; Jandke, M.; Strohriegl, P. *Synth. Met*. **1997**, *91*, 223−228.

(11) (a) Agrawal, A. K.; Jenekhe, S. A. *Macromolecules* **1991**, *24*, 6806−6808. (b) Agrawal, A. K.; Jenekhe, S. A. *Macromolecules* **1993**, *26*, 895−905. (c) Song, S. J.; Cho, S. J.; Park, D. K.; Kwon, T. W.; Jenekhe, S. A. *Tetrahedron Lett.* **2002**, *44*, 255−257. (d) Agrawal, A. K.; Jenekhe, S. A. *Chem. Mater*. **1992**, *4*, 95−104.

(12) (a) Zhu, Y.; Alam, M. M.; Jenekhe, S. A. *Macromolecules* **2003**, *36*, 8958−8968. (b) Zhu, Y.; Alam, M. M.; Jenekhe, S. A. *Macromolecules* **2002**, *35*, 9844−9846.

(13) (a) Zhang, X.; Shetty, A. S.; Jenekhe, S. A. *Macromolecules* **1999**, *32*, 7422−7429. (b) Tonzola, C. J.; Alam, M. M.; Jenekhe, S. A. *Adv. Mater*. **2002**, *14*, 1086−1090.

(14) (a) Zhang, X.; Jenekhe, S. A. *Macromolecules* **2000**, *33*, 2069−2082. (b) Jenekhe, S. A.; Zhang, X.; Chen, X. L.; Choong, V.-E.; Gao, Y.; Hsieh, B. R. *Chem. Mater*. **1997**, *9*, 409−412.

(15) (a) Lai, Y. L.; Kong, X. X.; Jenekhe, S. A.; Bard, A. J. *J. Am. Chem. Soc*. **2003**, *125*, 12631−12639. (b) Lai, Y. L.; Fabrizio, E. F.; Lu, L.; Jenekhe, S. A.; Bard, A. J. *J. Am. Chem. Soc*. **2001**, *123*, 9112−9118.

(16) Agrawal, A. K.; Jenekhe, S. A. Vanherzeele, H.; Meth, J. S. *J. Phys. Chem*. **1992**, *96*, 2837−2843.

(17) Miller, L. L.; Duan, R. G.; Tully, D. C.; Tomalia, D. A. *J. Am. Chem. Soc*. **1997**, *119*, 1005−1010.

Chart 2. Schematic of Peripheral Electron-Accepting Groups in Dendrimers

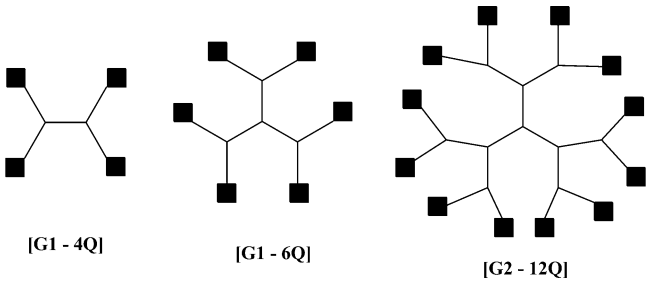

Chart 3. Chemical Structures of [G1]-CHO Dendron (4) and [G2]-CHO Dendron (5)

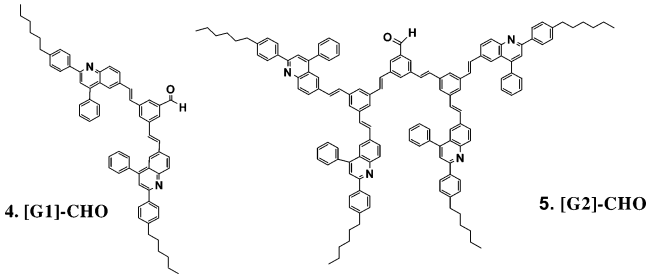

Scheme 1. Synthesis of [G1]-CHO Dendrons (4)

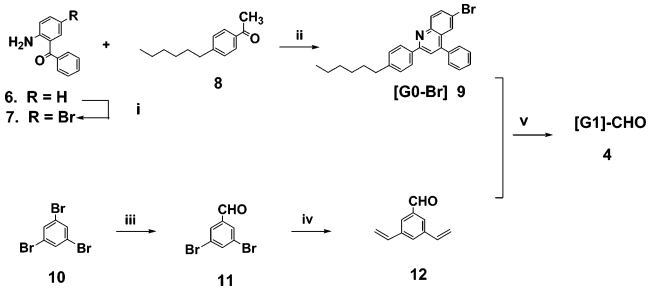

Reagents and conditions: (i) $(Bu)_4NBr_3$; (ii) diphenyl phosphate; (iii) *n*-BuLi/Et_2O, −78 °C, DMF; (iv) tributyl(vinyl)tin, palladium (II) acetate; (v) TBAB, K_2CO_3, $Pd(OAc)_2$, DMF.

nylene linkages were achieved by using a modified Heck type reaction.[19] To increase the solubility of the dendrimers (especially higher generations) in common organic solvents, *n*-hexyl alkyl chain was introduced. As shown in Scheme 1, the first step in the synthesis of **4** involves bromination of commercially available 2-aminobenzophenone (**6**) to obtain **7** with 52% yield in the presence of tetrabutylammonium tribromide/$CHCl_3$. Friedlander quinoline synthesis[11] by reacting 6-bromo-2-aminophenone (**7**) and 4-*n*-hexylacetophenone (**8**) in the presence of diphenyl phosphate (DPP) at 145 °C gave [G0]-Br (**9**) with 65% yield. 3,5-Divinylbenzaldehyde (**12**) was prepared by monoformylation of 1,3,5-tribromobenzene (**10**) followed by Stille coupling reaction in two steps using the procedure previously described in the literature.[20] The coupling reaction between [G0]-Br (**9**) and **12** gave the [G1]-CHO dendron (**4**) with 42% yield. [G1]-CHO (**4**) showed strong fluorescence in solution under UV light and was highly soluble in many common organic solvents such as ethyl acetate, $CHCl_3$, CH_2Cl_2, THF, and toluene.

Scheme 2. Synthesis of [G1-4Q] Dendrimer (1) and [G1-6Q] Dendrimer (2)

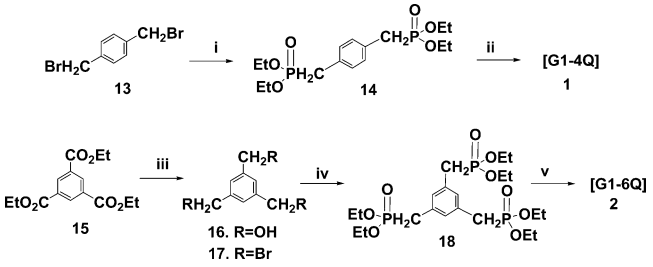

Reagents and conditions: (i) 2.2 equiv $P(OEt)_3$, reflux; (ii) [G1]-CHO, 2.9 equiv $KOC(CH_3)_3$, THF; (iii) borane−methyl sulfide complex/PBr_3; (iv) 3.3 equiv $P(OEt)_3$, reflux; (v) [G1]-CHO, 5.0 equiv $KOC(CH_3)_3$, THF.

Scheme 3. Synthesis of [G2]-CHO Dendron (5) and [G2-12Q] Dendrimer (3)

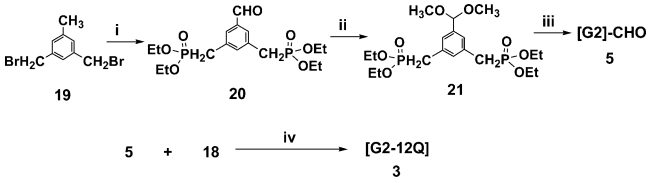

Reagents and conditions: (i) 2.2 equiv $P(OEt)_3$, reflux/NBS, AIBN, CCl_4/iron powder, reflux/aq HCl/neutralization; (ii) trimethyl orthoformate, Dowex 50W-X8, methanol, reflux, Na_2CO_3; (iii) [G1]-CHO, 2.2 equiv $KOC(CH_3)_3$, THF; (iv) 5 equiv $KOC(CH_3)_3$, THF.

The convergent syntheses of generation-one dendrimers [G1-4Q] and [G1-6Q] are shown in Scheme 2. The core reagents, [4-(diethoxy-phosphorylmethyl)-benzyl]-phosphonic acid diethyl ester (**14**) and triphosphonate ester (**18**), were prepared from 1,4-di(bromomethyl)-benzene (**13**) and 1,3,5-benzenetricarboxylate (**15**), respectively, according to previously described procedures.[21] Horner−Wadsworth−Emmons coupling reaction between 2.2 equiv of [G1]-CHO (**4**) and one equiv of 1,4-diphosphate **14** in the presence of $KO(CH_3)_3$/THF led to the conjugated poly(phenylenevinylene) dendrimer [G1-4Q] (**1**) which contains four diphenylquinoline (Q) moieties. In a similar manner, emissive [G1-6Q] dendrimer (**2**) which contains six diphenylquinoline groups was prepared from 3.3 equiv of [G1]-CHO (**4**) and one equiv of 1,3,5-triphosphate (**18**).

The next generation dendron [G2]-CHO (**5**) was prepared by Horner−Wadsworth−Emmons coupling reaction between masked diphosphate core reagent, tetraethyl 5-methoxymethyl-1,3-phenylenebis (methylenephosphonate) (**21**), and [G1]-CHO (**4**) as shown in Scheme 3. Compound **21** was prepared from 1,3-bis-(bromomethyl)-5-methylbenzene (**19**) similar to the literature procedure.[21] The focus point of dimethoxy acetal compound **21** is that it could be readily hydro-

(18) (a) Meier, H.; Lehmann, M. *Angew. Chem., Int. Ed.* **1998**, *37*, 643−645. (b) Lehmann, M.; Schartel, B.; Hennecke, M.; Meier, H. *Tetrahedron* **1999**, *55*, 13377−13394. (c) Pillow, J. N. G.; Halim, M.; Lupton, J. M.; Burn, P. L.; Samuel, I. D. W. *Macromolecules* **1999**, *32*, 5985−5993. (d) Palsson, L.-O.; Beavington, R.; Frampton, M. J.; Lupton, J. M.; Magennis, S. W.; Markham, J. P. J.; Pillow, J. N. G.; Burn, P. L.; Samuel, I. D. W. *Macromolecules* **2002**, *35*, 7891−7901.

(19) Diéz-Barra, E.; Garcia-Martinez, J.; Merino, S.; Rey, R.; Rodríguez-López, J.; Sanchez-Verdú, P.; Tejeda, J. *J. Org. Chem.* **2001**, *66*, 5664−5670.

(20) Deb, S. K.; Maddux, T. M.; Yu, L. *J. Am. Chem. Soc.* **1997**, *119*, 9079−9080.

(21) Meier, H.; Lehmann, M.; Kob, U. *Chem. Eur. J.* **2000**, *6*, 2462−2469.

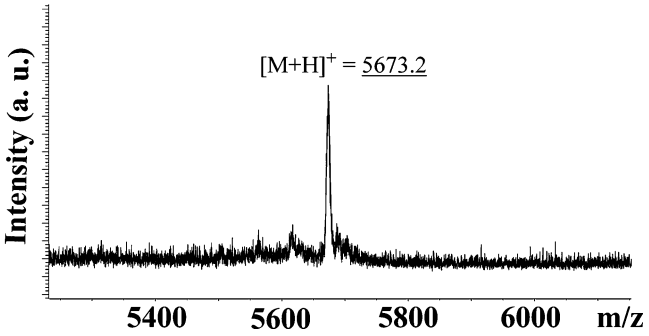

Figure 1. MALDI -TOF mass spectrum of [G2-12Q] dendrimer (**3**).

lyzed to regenerate the active aldehyde **5**. Subsequently, 3.3 equiv of [G2]-CHO (**5**) was reacted with one equiv of **18** via the Horner−Wadsworth−Emmons reaction to afford the [G2-12Q] dendrimer (**3**) (Scheme 3). The [G2-12Q] dendrimer (**3**) was highly soluble in $CHCl_3$, CH_2Cl_2, THF, or ethyl acetate. This is presumably in part because of the hydrophobic hexyl chains attached to the peripheral quinoline moieties.

All dendrimers and dendrons were characterized by ^1H and ^{13}C NMR spectra, high-resolution mass spectra, and matrix-assisted laser desorption time-of-flight (MALDI-TOF) mass spectra (see Supporting Information). [G1]-CHO (**4**) and [G2]-CHO (**5**) dendrons both possess a proton chemical shift at 10.03 and 10.09 ppm, respectively, which prove the formyl hydrogen. ^{13}C NMR spectra of the CHO focused dendrons showed clear peaks at 192.19 and 192.21 ppm which are due to the presence of aldehyde functionality. The disappearance of aldehyde peak and increased integration values of aromatic protons in the ^1H NMR spectra of the [G1-4Q], [G1-6Q], and [G2-12Q] dendrimers prove the successful coupling reaction between the respective aldehyde focused dendrons (**4** or **5**) and the core reagents (**14** and **18**). ^1H NMR spectra of the dendrimers showed the correct ratio of aliphatic (0.91−2.68 ppm) and aromatic protons (8.35−6.80 ppm). ^{13}C NMR spectra of the dendrimers, **1**, **2**, and **3**, showed complicated peaks in the range of 115−160 ppm due to the different environments of carbons in the aromatic rings of the dendrimers. However, the six aliphatic peaks in all cases can be clearly assigned and they confirm the purity of each dendrimer. Additional definitive evidence for the dendrimer molecular structures was obtained from MALDI-TOF mass spectra. The deviation between the calculated and experimentally measured *m/z* values was no more than one mass unit. For example, the molecular formula of [G2-12Q] is $C_{426}H_{384}N_{12}$. The calculated average for the peak of the molecular ion [M + H] is 5672.8 and we obtained the value 5673.2. The MALDI-TOF mass spectrum of [G2-12Q] dendrimer (**3**) is shown in Figure 1. The other two dendrimers (**1** and **2**) also showed the correct molecular ion peaks consistent with the calculated molecular weights (see Supporting Information).

Electrochemical Properties. The redox properties of dendrimers **1**−**3** were characterized by cyclic voltammetry. Typical cyclic voltammograms (CVs) in the −2.4 V to 1.8 V (vs SCE) potential range are shown in Figure 2 for thin films of dendrimer **1** coated on Pt wire electrodes. These CVs and that for **2** showed that the

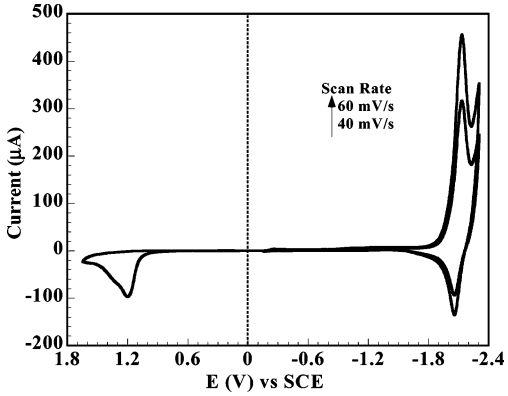

Figure 2. Cyclic voltammograms of [G1-4Q] dendrimer (**1**). Thin films were coated on Pt wire electrode using 0.1 M $TBAPF_6$ as supporting electrolyte in acetonitrile.

Table 1. Electrochemical Properties of Dendrimers[a]

cmpd	$E_{red}^{o'}$ (V)	E_{red}^{onset} (V)	EA (eV)	E_{ox}^{peak} (V)	E_{ox}^{onset} (V)	IP (eV)	E_g^{el} (eV)
[G1-4Q]	−2.08	−1.88	2.52	1.20	0.95	5.35	2.83
[G1-6Q]	−2.02	−1.86	2.55	1.26	1.00	5.40	2.85
[G2-12Q]	−1.99	−1.85	2.55	1.32	1.05	5.45	2.90

[a] All potentials are vs SCE reference.

dendrimers have a quasi-reversible reduction (n-type doping) but an irreversible oxidation. This general feature of the electrochemistry of the dendrimers is very similar to previously reported CVs of linear chain conjugated polyquinolines.[12,22] The formal potential (E°′) and other electrochemical data for **1**−**3** are summarized in Table 1. The E°′ value for reduction was ca. −2.0 V for all three dendrimers. The formal potential for reduction of these dendrimers is 0.2−0.3 V more negative compared to related linear chain conjugated polyquinolines[12,22] and about 0.1 V more positive than the value for 4-phenylquinoline small molecule.[15] The reason for these differences is because of the smaller conjugation length of the effective electroactive chromophore in the dendrimers (Chart 1), compared to the conjugated linear polyquinolines. The electroactive chromophore of the dendrimer is in turn larger than 4-phenylquinoline. We note that poly(phenylenevinylene) (distyrylbenzene core) dendrimers, without the present diphenylquinoline peripheral groups, have no detectable reduction waves in the range 0 to −2.4 V (vs SCE).[23] The observed reduction of dendrimers **1**−**3** is thus due to the diphenylquinoline peripheral groups, which are the designed electron-acceptor sites in the dendrimers.

The onset reduction potentials (E_{red}^{onset}) and the onset oxidation potentials (E_{ox}^{onset}) of dendrimers **1** − **3** were largely independent of generation or size (Table 1). The electron affinities (EA or LUMO levels) derived from the onset reduction potentials were very close for all three dendrimers, 2.52−2.55 eV; these are based on −4.4 eV as the SCE energy level relative to vacuum (EA = E_{red}^{onset} + 4.4 eV).[22] Similarly estimated ionization potentials (IP = E_{ox}^{onset} + 4.4 eV) were 5.35−5.45 eV

(22) (a) Agrawal, A. K.; Jenekhe, S. A. *Chem. Mater*. **1996**, *8*, 579−589. (b) Tonzola, C. J.; Alam, M. M.; Kaminsky, W.; Jenekhe, S. A. *J. Am. Chem. Soc*. **2003**, *125*, 13548−13558.

(23) (a) Frampton, M. J.; Beavington, R.; Lupton, J. M.; Samuel, I. D. W.; Burn, P. L. *Synth. Met*. **2001**, *121*, 1671−1672. (b) Schenk, R.; Gregorius, H.; Meerholz, K.; Heinze, J.; Mullen, K. *J. Am. Chem. Soc*. **1991**, *113*, 2634−2647.

Table 2. Photophysical Properties of Dendrimers

cmpd	λ_{max}^{Abs} (soln) (nm)	ϵ (10^5 M^{-1} cm^{-1})	λ_{max}^{Em} (soln) (nm)	ϕ_f (soln)	λ_{max}^{Abs} (film) (nm)	E_g^{opt} (eV)	λ_{max}^{Em} (film) (nm)	ϕ_f (film)
[G1-4Q]	360	0.93	414	0.69	364	2.85	532	0.04
[G1-6Q]	353	1.41	414	0.84	360	2.85	520	0.03
[G2-12Q]	353	3.28	414	0.87	355	2.85	534	0.03

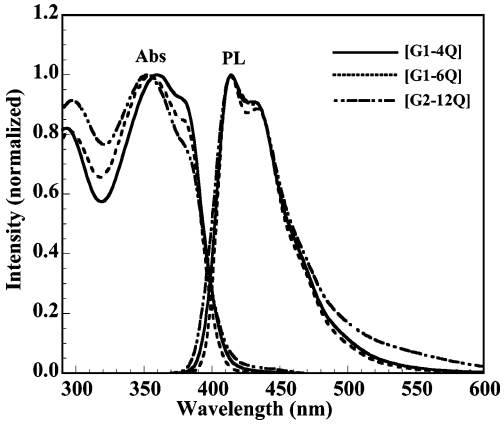

Figure 3. Absorption and PL emission spectra of dendrimers in dilute (3×10^{-6} M) toluene solutions. Excitation wavelength for PL spectra was 360 nm.

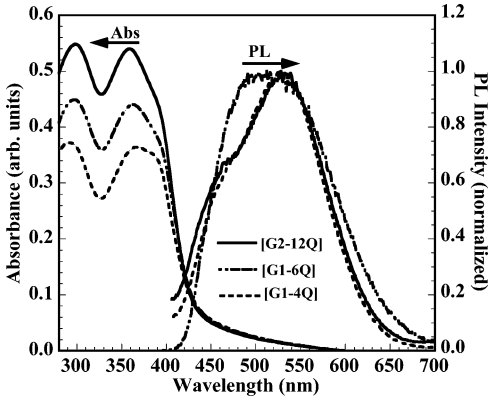

Figure 4. Absorption and PL emission spectra of dendrimer thin films spin coated from chloroform solutions. Excitation wavelength for PL spectra was 370 nm.

(Table 1). The related electrochemical band gap (E_g^{el}) was 2.83−2.90 eV for dendrimers **1**−**3**. Although the EA values of these dendrimers are about 0.1−0.3 eV smaller than those of linear chain conjugated polyquinolines already found to be good electron-transport materials for organic LEDs,[12−14] the many electron-acceptor sites per dendrimer molecule and the nonlinear spatial distribution of the electron-acceptor sites suggest that these dendrimers are attractive as electron-transport materials for LEDs.

Photophysical Properties. Absorption spectra of dendrimers **1**−**3** in toluene solution are shown in Figure 3. Dendrimer **1** has absorption maximum at 360 nm with a shoulder peak at 380 nm. Dendrimers **2** and **3** have identical absorption maxima (λ_{max}) at 353 nm and the same shoulder peak at 380 nm as in **1**. The absorption bands of the dendrimers in the range 250−420 nm are broader than those of the isolated diphenylquinoline moiety, which absorbs in the 250−360 nm range, or the distyrylbenzene (or phenylenevinylene) core which absorbs in the range 270−390 nm with a peak at 350 nm. This observation suggests that both chromophores, distyrylbenzene core and peripheral 2,4-diphenylquinoline moiety, contribute to the broad absorption bands of these dendrimers. The lowest energy absorption bands of the dendrimers are due to $\pi-\pi^*$ transitions by virtue of their large molar extinction coefficients ($\epsilon \sim 10^5$ $M^{-1}cm^{-1}$; Table 2). A slight blue shift in the absorption maxima of dendrimers **2** and **3** compared to that of dendrimer **1** was observed, and this is likely due to a decrease in conjugation length because of steric hindrance of the diphenylquinoline moieties in dendrimers **2** and **3** compared to dendrimer **1**. A similar phenomenon has been previously observed for other meta-linked stilbene-based dendrimers.[18]

The dilute-solution (3×10^{-6} M) photoluminescence (PL) spectra of dendrimers **1**−**3** in toluene are shown in Figure 3. The dendrimers emit blue light with similar structured emission bands and emission maxima of λ_{max} = 414 nm. The PL spectra of the dendrimers are shifted to the red by about 20 nm compared to the PL spectrum of distyrylbenzene chromophore core which has an emission maximum at 395 nm. On the other hand the peripheral 2,4-diphenylquinoline moiety has a PL emission peak at 413 nm, which is identical to the PL emission peak of dendrimers **1**−**3**, suggesting that the PL emission of the dendrimers comes from the peripheral diphenylquinoline moieties. The Stokes shifts are 3623 cm^{-1} (0.45 eV) for **1** and 4174 cm^{-1} (0.52 eV) for **2** and **3**. The observed large Stokes shifts suggest that the excited-state relaxation to a more planar conformation is much larger in dendrimers **2** and **3** compared to **1**. The PL quantum yield (ϕ_f) of compounds **1**−**3** in dilute solution in toluene was very high, ranging from 0.69 for **1** to 0.87 for **3** (Table 2).

The thin film optical absorption spectra of dendrimers **1**−**3** are shown in Figure 4. Both core and peripheral chromophores contribute to the solid-state absorption bands of the dendrimers similar to the solution ones. The solid-state absorption bands are, however, broader and red shifted by about 7−10 nm compared to the solution spectra, suggesting that there is a slight increase in conjugation length in the solid state. Such an increase in conjugation length is expected from the more planar conformations due to the π-stacking/aggregation in the solid state. Optical band gaps (E_g^{opt}) determined from the absorption edge of the solid-state spectra are given in Table 2. All three dendrimers have identical optical band gaps of 2.85 eV, which is in good agreement with those determined from cyclic voltammetry (Table 1).

The PL emission spectra of thin films of **1**−**3** are also shown in Figure 4. The solid-state emission bands of the dendrimers are very broad and featureless. Also, compared to the solution PL spectra these thin film PL spectra are red shifted by 116−120 nm (Table 2). In contrast to the PL emission spectra in solution which have full width at half-maximum (fwhm) values of only 54−58 nm, the thin film PL emission spectra have fwhm values of 136−147 nm. We propose that the absence of monochromatic shift with size in the dendrimer thin-

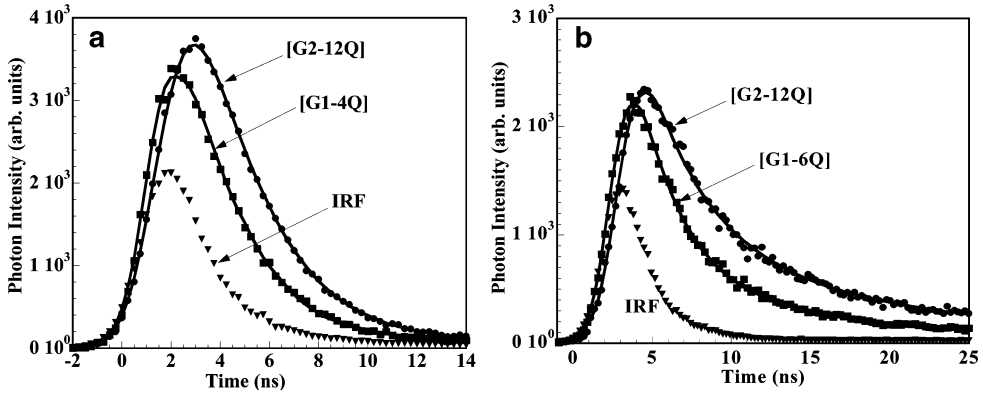

Figure 5. Representative time-resolved PL decay curves of dendrimers: (a) in toluene solution and (b) as thin films. Solid lines are the fit curves. Excitation at 380 nm and PL decay monitored at corresponding PL peaks.

Table 3. PL Decay Lifetime of Dendrimers in Solution and as Thin Films

cmpd	τ_1 (ns)	τ_2 (ns)	amplitude (% τ_1/τ_2)	χ^2
[G1-4Q] (toluene)	1.4		100	1.28
[G1-6Q] (toluene)	1.6		100	1.31
[G2-12Q] (toluene)	1.6		100	0.94
[G1-4Q] (film)	10.5	1.30	80/20	1.20
[G1-6Q] (film)	7.7	1.10	89/11	1.40
[G2-12Q] (film)	7.7	1.20	75/25	1.11

film PL emission is likely due to broad, structureless, intermolecular excimer emission[24] which is a well-known phenomenon in conjugated molecules and polymers. The PL emission quantum yield in the thin films was poor, confirming the intermolecular nature of the emission.

To further explore the photophysics of the new dendrimers we obtained PL decay dynamics information. The PL decay dynamics of dendrimers **1**−**3** are exemplified by the PL decay curves and data shown in Figure 5 and Table 3. The PL decay dynamics of the dendrimers in toluene solution was well described by a single-exponential fit (Figure 5a), yielding lifetimes of 1.4 ns for dendrimer **1** and 1.6 ns for dendrimers **2** and **3** (Table 3). The PL decay lifetimes of the dendrimers in solid films were best described by two exponential fits (Figure 5b). All three dendrimer solid films have rather long-lived excited-state species with dominant fluorescence lifetimes in the range 7.7−10.5 ns (Table 3). These PL decay dynamics results are in accord with our interpretation of the steady-state emission in thin films as due to intermolecular excimers.[24]

Light-Emitting Diodes. We used dendrimers **1**−**3** in light-emitting diodes (LEDs) both as the emissive materials in single-layer diodes and as the electron-transport materials in bilayer diodes. The former devices provided information on the intrinsic electroluminescence (EL) of the dendrimers and the bilayer diodes allowed the evaluation of the electron-transport properties of the dendrimers. To investigate the EL properties of **1**−**3** we fabricated LEDs using poly(ethylenedioxythiophene)/poly(styrene sulfonic acid) (PEDOT) thin film on indium tin oxide (ITO) as the anode, the spin-coated dendrimer as the emissive layer, and aluminum as the cathode: ITO/PEDOT/**1**−**3**/Al. The EL spectra of **1**−**3** are shown in Figure 6a. All three dendrimers exhibited yellow electroluminescence with peaks at 535−550 nm. The broad structureless line shapes of the EL spectra are similar to those of the PL spectra (Figure 4) and are indicative of intermolecular excimer emission from the aggregated dendrimers. The device characteristics of the ITO/PEDOT/**1**−**3**/Al LEDs are shown in Table 4. The turn-on voltage (electric field) of these diodes was 8.5−9.5 V (∼1.1 × 10^6 V/cm). The maximum brightness of the devices was 22−56 cd/m^2 when using **1**−**3** as the emissive materials. The corresponding external quantum efficiency (EQE) was also low (0.009−0.01%; Table 4). The poor performance of the dendrimers as emissive EL materials is consistent with their low solid-state PL quantum yields. In addition, imbalanced charge transport through the dendrimers and the energy barrier (∼0.35−0.45 eV) for hole injection from PEDOT into **1**−**3** partly explain the poor performance of the single-layer diodes.

To understand the limitations of the imbalanced charge transport through the dendrimers and the energy barrier for hole injection into dendrimers **1**−**3**, we incorporated a thin layer (30 nm) of poly(*N*-vinylcarbazole) (PVK) between the PEDOT and **1**−**3** in LEDs. These ITO/PEDOT/PVK/**1**−**3**/Al diodes also exhibited yellow electroluminescence with EL spectral line shapes identical to those of the ITO/PEDOT/**1**−**3**/Al diodes shown in Figure 6a. The EL emission of these LEDs including a PVK hole-transport layer comes from dendrimers **1**−**3**. Figure 6b shows representative current−voltage and luminance−voltage curves of one such diode, ITO/PEDOT/PVK/**3**/Al. These devices indeed showed improvement in both brightness and efficiency as shown in Table 4. The brightness and external quantum efficiency values nearly triple to 157 cd/m^2 and 0.23%, respectively, compared to those without the PVK. The large ionization potential (IP) of the dendrimers, and thus hole-blocking properties, in combination with their moderate electron affinities (EA) suggest that they are very promising as electron-transport materials in organic and polymer LEDs.

Dendrimers **1**−**3** were used as electron-transport materials in polymer LEDs in conjunction with poly(2-methoxy-5-(2′-ethyl-hexyloxy)-1,4-phenylene vinylene) (MEH-PPV) as the emissive material. The bilayer ITO/PEDOT/MEH-PPV/**1**−**3**/Al diodes were fabricated by sequential spin-coating of the MEH-PPV layer followed by spin coating of the dendrimer layer from formic acid solution on top of the MEH-PPV layer. The film thick-

(24) (a) Jenekhe, S. A.; Osaheni, J. A. *Science* **1994**, *265*, 765−768. (b) Osaheni, J. A.; Jenekhe, S. A. *Macromolecules* **1994**, *27*, 739−742.

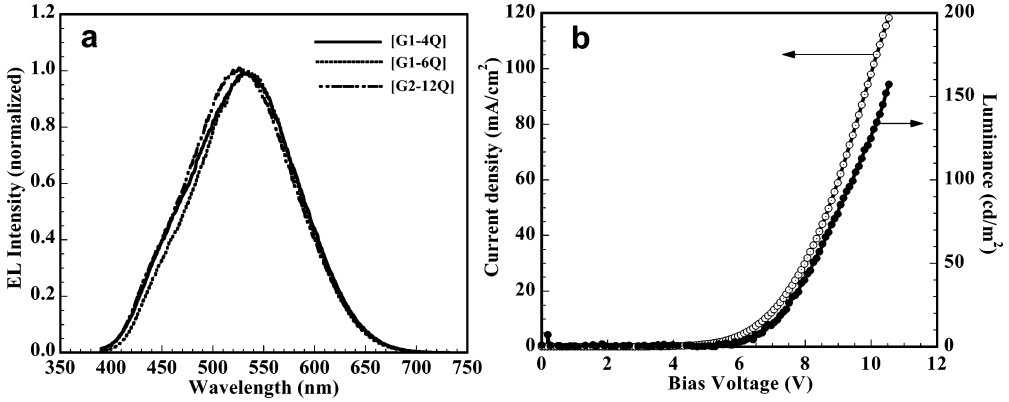

Figure 6. (a) Electroluminescence spectra of ITO/PEDOT/dendrimer/Al diodes. (b) Current−voltage−luminance curves of ITO/PVK/[G2-12Q]/Al diodes.

Table 4. Electroluminescent Device Properties of Dendrimers

LED configuration[a]	V_{on}[b] (V)	L_{max}[c] (cd/m^2)	J_{max} (mA/cm^2)	V_{max} (V)	EQE[d] (%)
[G1-4Q]	9.0	22	182	14.0	0.009
[G1-6Q]	8.5	41	209	15.0	0.01
[G2-12Q]	9.5	56	350	17.0	0.01
PVK/[G1-4Q]	7.5	39	169	12.0	0.03
PVK/[G1-6Q]	7.0	98	137	14.0	0.07
PVK/[G2-12Q]	5.5	157	118	11.0	0.23
MEH-PPV	4.0	66	500	7.5	0.03
MEH-PPV/[G1-4Q]	4.0	745	470	10.0	0.38
					0.50 (9 V)[e]
MEH-PPV/[G1-6Q]	3.5	1328	408	11.5	0.9
					2.5 (6.5 V)[e]
MEH-PPV/[G2-12Q]	3.0	1983	216	10.0	2.6
					5.0 (6.5 V)[e]

[a] ITO/PEDOT/[G*x*-*y*Q]/Al, ITO/PEDOT/PVK/[G*x*-*y*Q]/Al, ITO/PEDOT/MEH-PPV/Al, or ITO/PEDOT/MEH-PPV/**1**−**3**/Al. [b] Turn-on voltage. [c] Brightness at maximum bias voltage. [d] External quantum efficiency at maximum bias voltage. [e] Maximum external quantum efficiency at the bias voltage shown in parentheses.

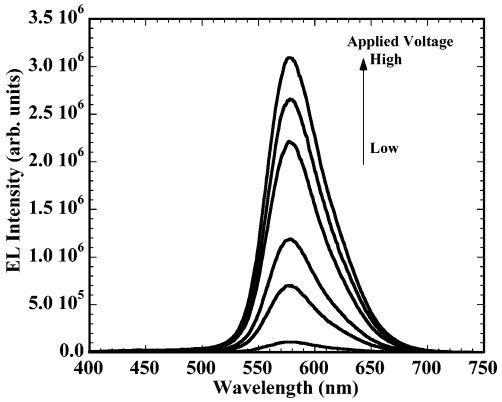

Figure 7. Electroluminescence spectra of ITO/PEDOT/MEH-PPV/[G2-12Q]/Al diodes at varying forward bias voltages.

ness of **1**−**3** as electron-transport layers in these diodes was 55−60 nm. The typical EL spectra from these bilayer LEDs are shown in Figure 7 for the ITO/PEDOT/MEH-PPV/**3**/Al diode. At all forward-applied bias-voltages, only the characteristic orange-red emission of MEH-PPV with an EL emission maximum at 580 nm was seen. Similar EL spectra were obtained for other bilayer LEDs. These EL spectra results confirmed that dendrimers **1**−**3** functioned as electron-transport materials in the devices.

The current−voltage and luminance-voltage characteristics of the MEH-PPV diodes using **1**−**3** as electron-transport materials are shown in Figure 8. The LED performance data are summarized in Table 4. The turn-on voltage (electric field) of these LEDs was 3.0−4.0 V (3.0−4.0 × 10^5 V/cm). The maximum brightness of the LEDs was in the range of 745 cd/m^2 for **1** to 1983 cd/m^2 for **3**. All the MEH-PPV/dendrimer (**1**−**3**) bilayer LEDs operated at a reduced turn-on voltage compared to that of the single-layer MEH-PPV or dendrimer diodes, suggesting improved electron injection and transport compared to those of the single-layer diodes. The luminance of the bilayer LEDs using a dendrimer as an electron-transport layer was also substantially enhanced compared to that of the single-layer MEH-PPV or dendrimer diodes (Table 4). The luminance values are factors of 11−35 times greater than that of the single-layer MEH-PPV or dendrimer diodes.

In terms of efficiency, the reference external quantum efficiency of the single-layer MEH-PPV diode was 0.03%. The external quantum efficiency of the bilayer MEH-PPV/dendrimer devices varied from 0.38 to 5.0% (photons/electron) depending on the dendrimer used as an electron-transport layer. The MEH-PPV/**3** diode showed the best performance with a maximum external quantum efficiency of 5.0% (photons/electron), power efficiency of 1.3 lm/W and device efficiency of 1.5 cd/A at 6.5 V, and a brightness level of 240 cd/m^2 (Table 4). The MEH-PPV/**2** diode had a maximum external quantum efficiency of 2.5%, power efficiency of 0.5 lm/W and device efficiency of 0.6 cd/A at 6.5 V, and a brightness level of 190 cd/m^2 (Table 4). These results represent factors of 87−167 enhancements over the single-layer MEH-PPV diode. Incorporation of a dendrimer as an electron-transport layer has thus resulted in a large improvement in the performance (lower turn-on voltage, higher luminance, and higher EL efficiency) of MEH-PPV-based LEDs. On the basis of the external quantum efficiency of the LEDs, the decreasing order of effectiveness as an electron-transport layer of the dendrimers is **3** > **2** > **1**. These results show that the higher the generation, the better the dendrimer is as an electron-transport and hole-blocking material in LEDs. Furthermore, the performance as an electron-transport layer improves substantially with the number of peripheral diphenylquinoline moieties in the dendrimer. Considering the LUMO levels of the three dendrimers are essentially identical, the main variable that explains the

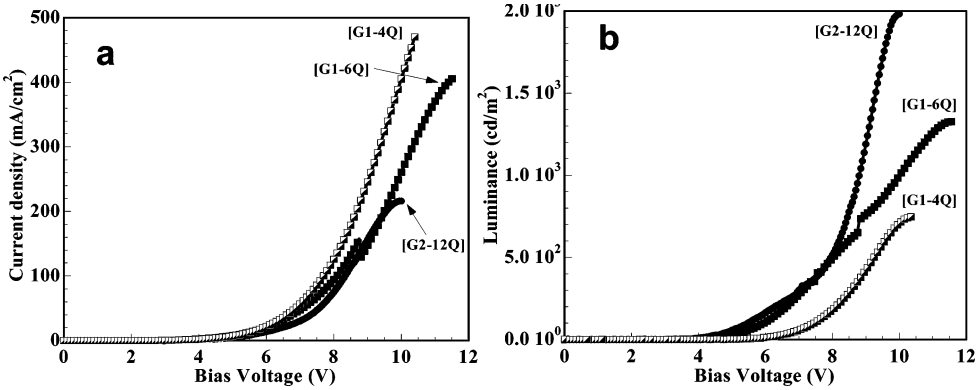

Figure 8. (a) Current−voltage curves and (b) luminance−voltage curves for three LEDs using dendrimers **1**−**3** as the electron-transport layer and MEH-PPV as the emissive layer in ITO/PEDOT/MEH-PPV/**1**−**3**/Al.

results appears to be electron mobility which should be in the decreasing order [G2-12Q] > [G1-6Q] > [G1-4Q]. An independent direct measurement of electron mobility in these dendrimers would be very useful for a detailed understanding of the relationship of charge transport to EL device performance. We note that our findings are different from those of electroactive-core dendrimers where hole mobility as well as LED device performance decreased with increasing generation.[6]

Electroactive and emissive dendrimers have been extensively studied by different groups in the past several years, including their applications in organic LEDs.[1−10] However, to our knowledge, the present dendrimers are the first designed and demonstrated as electron-transport materials for solution-processed polymer LEDs. The present results show that the bilayer dendrimer LEDs of the type ITO/PEDOT/MEH-PPV/**1**−**3**/Al have far better device performance than that of any previously reported dendrimer-based LEDs. On the basis of the requirements for efficient multicomponent-blend LEDs,[25] we believe that the novel dendrimers **1**−**3** could also be used as electron-transport and hole-blocking materials in such device architectures.

Conclusions

We have described the efficient convergent synthesis and detailed characterization of novel electron-acceptor and luminescent dendrimers [G1-4Q], [G1-6Q], and [G2-12Q], and related [G1]-CHO and [G2]-CHO dendrons. Cyclic voltammetric studies showed that the new dendrimers can be reduced quasi reversibly at the electron-acceptor diphenylquinoline peripheral sites. In solution, all three dendrimers emit blue light with very high fluorescence quantum yields (0.69−0.87) and fluorescence lifetimes of 1.4−1.6 ns. However, due to strong aggregation in thin films they emit yellow light with poor quantum yields. The dendrimers exhibit yellow electroluminescence, the brightness and external quantum efficiency of which increased with generation and the number of electron-acceptor peripheral groups. Use of the dendrimers as electron-transport materials for MEH-PPV-based LEDs showed generation-dependent substantial enhancement of device performance, reaching an external quantum efficiency of 5.0% and a luminescence of 2000 cd/m^2 for the [G2-12Q] dendrimer. These results demonstrate that the series of new n-type dendrimers can be used as electron-transport and hole-blocking materials for the construction of more efficient and stable LEDs.

Experimental Section

Materials and Methods. Diphenyl phosphate (DPP), poly(*N*-vinyl carbazole) (PVK), and poly(ethylenedioxythiophene)/poly(styrenesulfonic acid) (PEDOT; solution in water) were used as received from Aldrich. Poly(2-methoxy-5-(2′-ethylhexyloxy)-*p*-phenylene vinylene) (MEH-PPV, $M_w \approx 85\,000$) was purchased from American Dye Source, Inc. Potassium carbonate was dried and stored in an oven at 130 °C. Tetrahydrofuran (THF: 99.9%) and chloroform were either used as supplied or purified by standard techniques. All reactions requiring anhydrous condition were performed in oven-dried glassware under argon or N_2 atmosphere. TLC was performed on precoated glass plate−silica gel 250-μm (Baker Si250F) with detection by UV light. Flash column chromatography was performed on silica gel (230−400 mesh). The ^{1}H NMR spectra were recorded on a Bruker-DRX499 at 499 MHz or a Bruker-AF301 at 300 MHz. ^{13}C NMR spectra were recorded on a Bruker-WM500 spectrometer at 500 MHz. The spectra were recorded using $CDCl_3$ as the solvent at room temperature. The solvent signals were used as internal standards for both ^{1}H NMR and ^{13}C NMR. Chemical shifts are given in ppm and referenced to internal tetramethylsilane (TMS, $\delta = 0$ ppm) standard. Matrix-assisted laser desorption time-of-flight mass spectra (MALDI-TOF MS) were recorded on a Biflex III instrument (Bruker Daltonics, Billerica, MA) equipped with a nitrogen laser (337 nm). Compounds to be analyzed were dissolved in dichloromethane and the MALDI probe was spotted with 1 mL of a 1:1 (v:v) mixture of sample and a saturated solution of a cyano-4-hydroxycinnamic acid (HCCA) in acetonitrile. The instrument was operated in the positive ion mode with an accelerating potential of 20 kV and an extraction delay of 500 ns. A spectrum was produced by collecting and averaging data generated from 50 laser pulses.

Cyclic Voltammetry. Cyclic voltammetry (CV) experiments were done on an EG&G Princeton Applied Research potentiostat/galvanostat (model 273A). A three-electrode cell was used in all experiments. Platinum wire electrodes were used as both counter and working electrodes and silver/silver ion (Ag in 0.1 M $AgNO_3$ solution, Bioanalytical System, Inc.) was used as a reference electrode. Ferrocene/ferrocenium (Fc/Fc^+) redox couple was used as an internal standard and the potential values thus obtained in reference to Ag/Ag^+ electrode were converted to the saturated calomel electrode (SCE) scale. The dendrimer was coated onto the Pt working electrode by dipping the Pt wire into the viscous dendrimer solution in $CHCl_3$ and then dried in a vacuum oven at 60 °C for 8 h. Acetonitrile (ultrapure, 99.93+%, <0.005% water) and tetrabutylammonium hexafluorophosphate ($TBAPF_6$) were ob-

(25) (a) Zhang, X.; Kale, D. M.; Jenekhe, S. A. *Macromolecules* **2002**, *35*, 382−393. (b) Alam, M. M.; Tonzola, C. J.; Jenekhe, S. A. *Macromolecules* **2003**, *36*, 6577−6587.

tained from Aldrich and used as received. An electrolyte solution of 0.1 M $TBAPF_6$ in acetonitrile was used in all experiments. All solutions in the three-electrode cell were purged with ultrahigh-purity N_2 for 10−15 min before each experiment and a blanket of N_2 was used during the experiment.

Photophysics. UV−vis spectra were recorded on a Perkin-Elmer Lambda 900 UV/VIS/NIR spectrophotometer. Photoluminescence spectra were measured on a PTI QuantaMaster model QM-2001-4 spectrofluorometer (Photon Technology International Inc., London, ON). Fluorescence quantum yields in solution were determined by using a perylene standard (10^{-6} M in toluene, $\phi_f = 87\%$).[26] Approximate relative fluorescence quantum efficiencies of the dendrimer thin films were determined by using a thin film of $\sim 10^{-3}$ M 9,10-diphenylanthracene in poly(methyl methacrylate) as a standard ($\phi_f = 83\%$).[13a,27] Time-resolved fluorescence decays of the dendrimers both in solution and in thin films were measured on a PTI model Q-10/A-611 StrobeMaster fluorescence lifetime spectrometer.[28a] The instrument utilizes a nanosecond flash lamp as an excitation source and a stroboscopic detection system. Dendrimers in solution were excited at a wavelength of 360 nm and in the thin films at 370 nm, and the fluorescence decay was monitored at the corresponding emission peak of each dendrimer. The decay curves were analyzed with a PTI TimeMaster Pro-software package by utilizing either a discrete 1 to 4 exponential fit using nonlinear least squares or the exponential series (ESM) lifetime distribution analysis.[28] Chi-square (χ^2) values and weighed residuals were used as the goodness-of-fit criteria.

Devices. Three types of LEDs were fabricated and characterized: ITO/PEDOT/**1**−**3**/Al, ITO/PEDOT/PVK/**1**−**3**/Al, and ITO/PEDOT/MEH-PPV/**1**−**3**/Al. The LEDs were fabricated by sequential spin coating of the layers onto cleaned ITO-coated glass substrates (see Supporting Information for detail). Electroluminescence (EL) spectra were measured on a PTI QuantaMaster model C-60/2000 spectrofluorometer. The electrical characteristics of the devices were measured on an HP4155A semiconductor parameter analyzer together with a Grasby S370 optometer equipped with a calibrated luminance sensor head. The EL quantum efficiencies of the diodes were measured by using procedures similar to those previously reported.[13,14] All the fabrications and measurements were done under ambient laboratory conditions at room temperature in air.

Synthesis of Core Reagents 14, 18, and 21. The synthesis of [4-(diethoxy-phosphorylmethyl)-benzyl]-phosphonic acid diethyl ester (**14**) using the Arbuzov reaction between 1,4-di-(bromomethyl)benzene (**13**) and triethyl phosphite was performed according to a procedure described in the literature[21] with 96.2% yield. A white solid recrystallized from hot hexane with minimum of methylene chloride (rf = 0.5, 5% MeOH/95% ethyl acetate). ^{1}H NMR (499 MHz, $CDCl_3$): δ 7.21 (s, 4H, Ar−*H*), 4.06−3.91 (q, 8H, O*CH*$_2$), 3.08 (d, 4H, P−*CH*$_2$, J = 20.2 Hz), 1.27−1.14 (12H, four *CH*$_3$). ^{13}C NMR ($CDCl_3$): δ 130.12, 61.79, 36.11, 29.89, 16.02 ppm.

Triphosphonate ester (**18**) was synthesized from commercially available triethyl 1,3,5-benzenetricarboxylate (**15**) via (3,5-bishydroxylemthyl-phenyl)-methanol (**16**) and 1,3,5-tris-bromomethyl benzene (**17**) in three steps. **16:** ^{1}H NMR (499 MHz, $CDCl_3$) δ 7.22 (s, 3H, Ar−*H*), 4.58 (s, 6H, Ar−*CH*$_2$). **17:** ^{1}H NMR (499 MHz, $CDCl_3$) δ 7.38 (s, 3H, Ar−*H*), 4.52 (s, 6H, Ar−*CH*$_2$Br). **18:** Yield 91%, viscous oil (rf = 0.15, 10% MeOH/ethyl acetate). ^{1}H NMR (499 MHz, $CDCl_3$) δ 7.14 (s, 3H, Ar−*H*), 4.12−4.03 (m, 12 H, six O*CH*$_2$), 3.14−3.10 (d, 6H, three P−*CH*$_2$, d, J = 21.9 Hz), 1.34−1.23 (18H, six *CH*$_3$). ^{13}C NMR ($CDCl_3$) δ 132.8, 130.1, 62.3, 32.9, 16.8 ppm.

Tetraethyl-5-methoxymethyl-1,3-phenylenebis (methylenephosphonate) (**21**) was prepared from commercially available 1,3-bis(bromomethyl)-5-methylbenzene (**19**) via tetraethyl-5-formyl-1,3-phenylene bis(methylenephosphonate) (**20**). **20:** ^{1}H NMR (499 MHz, $CDCl_3$) δ 10.00 (s, 1H, Ar−*CH*O), 7.73 (s, 2H, Ar−*H*), 7.54 (s, 1H, Ar−*H*), 4.06 (m, 8H, O*CH*$_2$), 3.24 (d, 4H, P *CH*$_2$, J = 21.8 Hz), 1.29 (t, 12H, CH_2*CH*$_3$). **21:** ^{1}H NMR (499 MHz, $CDCl_3$) δ 7.28 (s, 2H, Ar−*H*), 7.16 (s, 1H, Ar *H*), 5.38 (s, 1H, C*H*(OCH_3)$_2$), 4.06 (q, 8H, O*CH*$_2$), 3.28 (s, 6H, O*CH*$_3$), 3.18−3.14 (d, 4H, P−*CH*$_2$, J = 21.7 Hz), 1.27 (t, 12H, CH_2*CH*$_3$). ^{13}C NMR ($CDCl_3$): δ 138.9, 132.5, 131.5, 127.1, 103.1, 62.5, 52.9, 33.9, 16.8. Oil (yield 93%), rf = 0.28 (10% MeOH/ethyl acetate).

6-Bromo-2-(4-hexyl-phenyl)-4-phenyl-quinoline, [G0]-Br (9). (2-Amino-5-bromo-phenyl)-methanone (**7**) (34.7 g, 125.7 mmol, 1 equiv), 4-hexyl benzaldehyde (**8**) (28.3 g, 138.3 mmol, 1.1 equiv), and diphenyl phosphate (125.8 g, 502.9 mmol, 4 equiv) were mixed in a 500-mL glass reactor fitted with a mechanical stirrer, two glass inlets, and a sidearm. The reaction mixture was purged with argon for 15 min, and then the temperature was gradually raised to 90 °C under argon atmosphere for 1 h and then to 140 °C for 16 h. The mixture was then allowed to cool to room temperature. The reaction mixture was diluted with 1 L of diethyl ether, washed with 10% NaOH (2 × 500 mL), washed with distilled water (2 × 500 mL), and dried over anhydrous magnesium sulfate. After removal of solvent under reduced pressure, the product was purified by recrystallization from hot ethanol to give a white solid (36.4 g, 81.7 mmol, 65%); mp = 54 °C, rf = 0.79 (TLC eluent; 20% ethyl acetate/80% hexane, v/v). ^{1}H NMR (300 MHz, $CDCl_3$): δ 8.06−8.10 (m, 3H), 8.01−8.02 (d, 1H), 7.79−7.81 (m, 2H), 7.52−7.57 (m, 5H), 7.31−7.34 (d, 2H), 2.65−2.70 (t, 2H), 1.60−1.68 (m, 2H), 1.27−1.37 (m, 6H), 0.86−0.90 (t, 3H) ppm. ^{13}C NMR (75 MHz, $CDCl_3$): δ 157.68, 148.61, 147.85, 145.23, 138.20, 137.01, 133.30, 132.19, 129.85, 129.43, 129.21, 129.07, 128.16, 127.83, 127.31, 120.56, 120.34, 36.18, 32.13, 31.73, 29.33, 23.07, 14.51 ppm. HRMS: *m/z* Calcd for $C_{27}H_{26}$-BrN $[M + H]^+$, 445.4139; found, 445.4135.

Synthesis of 3,5-Divinylbenzaldehyde (12). Compound **12** was prepared by monoformylation of 1,3,5-tribromobenzene (**10**) (85%, rf = 0.3, 10% CH_2Cl_2 in hexane) followed by Stille coupling reaction of 3,5-dibromo-benzaldehye (**11**) (yield 62%, rf = 0.18, 20% CH_2Cl_2 in hexane) as described in the literature.[20] ^{1}H NMR (300 MHz, $CDCl_3$): δ 10.03 (s, 1H, ArC*H*O), 7.79 (s, 2H, two Ar−*H*), 7.65 (s, 1H, one Ar−*H*), 6.76 (m, 2H, two C*H*═CH_2), 5.89−5.86 (d, 2H, two trans C*H*═CH, J = 17.4 Hz), 5.39−5.38 (d, 2H, two cis C*H*═CH, J = 10.97 Hz). ^{13}C NMR (125 MHz): δ 192.49 (Ar−*C*HO), 139.14, 136.03, 135.67, 129.9, 127.02, 116.28.

Synthesis of [G1]-CHO (4). A round-bottomed flask (250 mL) was oven dried and cooled under argon atmosphere. 6-Bromo-2-(4-hexyl-phenyl)-4-phenyl-quinoline (**9**) (5.80 g, 13.09 mmol, 2.1 equiv), 3,5-divinylbenzaldehyde (**12**) (0.98 g, 6.23 mmol, 1.0 equiv), $Pd(OAc)_2$ (0.28 g, 1.24 mmol), tetra-*n*-butylammoniumbromide (2.52 g, 7.81 mmol), and K_2CO_3 (4.32 g, 31.01 mmol) were dissolved in DMF (17 mL). The reaction mixture was heated to 135 °C in an oil bath and stirred for 48 h in a dark environment (because of the photosensitivity of **12**). The DMF was then removed under reduced pressure and the residue was dissolved in $CHCl_3$ (500 mL) and extracted with water (100 mL × 3) and brine (100 mL × 2). The organic solution was dried using $MgSO_4$ and filtered. The crude product was purified by flash column chromatography. Rf = 0.35 (20% ethyl acetate in hexane) and further solidified using EtOH/$CHCl_3$ to give [G1]-CHO (**4**) (2.3 g, 2.62 mmol, and 42% yield). Mp = 113−115 °C. ^{1}H NMR (499 MHz, $CDCl_3$): δ 10.09 (s, 1H, C*H*O), 8.32−7.25 (m, 33H, Ar−*H*), 2.73−2.70 (t, 4H, Ar−*CH*$_2$), 1.69−1.59 (m, 4H, ArCH_2−*CH*$_2$), 1.36−1.34 (m, 12H, (*CH*$_2$)$_3$), 0.92 (t, 6H, terminal *CH*$_3$). ^{13}C NMR ($CDCl_3$): δ 192.19 (Ar−*CHO*), 156.97, 149.01, 138.68, 138.43, 137.30, 136.90, 134.46, 130.69, 130.58, 130.31, 129.64, 129.55, 129.05, 128.93, 127.71, 127.58, 127.50, 126.63, 126.49, 125.97, 125.12, 119.80, 35.86, 31.80, 31.40, 29.01, 22.69, 14.17 ppm. HRMS (FAB) *m/z* calcd for C_{65} H_{60} N_2O $[M + H]^+$, 885.478; found, 885.406.

Synthesis of G1-dendrimer [G1−4Q] (1). A round-bottomed flask (25 mL) was oven dried and cooled under argon

(26) Kavarnos, G. J.; Turro, N. J. *Chem. Rev*. **1986**, *86*, 401−449.
(27) (a) Osaheni, J. A.; Jenekhe, S. A. *J. Am. Chem. Soc*. **1995**, *117*, 7389−7398. (b) Jenekhe, S. A.; Lu, L.; Alam, M. M. *Macromolecules* **2001**, *34*, 7315−7324.
(28) (a) Sadlej-Sonsnowska, N.; Siemiarczuk, A. *J. Photochem. Photobiol., A* **2001**, *138*, 35−40. (b) Siemiarczuk, A.; Wagner, B. D.; Ware, W. R. *J. Phys. Chem*. **1990**, *94*, 1661−1669.

atmosphere. Potassium *t*-butoxide (0.17 g, 1.50 mmol, 2.9 equiv) was dissolved in 5 mL of THF under argon atmosphere at RT. A solution mixture of [G1]-CHO (**4**) (1.00 g, 1.13 mmol, 2.2 equiv) and bisphosphate (**14**) (0.19 g, 0.51 mmol, 1 equiv) in 15 mL of THF was added via a syringe. The yellow reaction mixture was stirred for 48 h at RT and then quenched with distilled water (1 mL), and THF was evaporated under reduced pressure. The residue was dissolved in $CHCl_3$ (150 mL) and the organic layer was washed with brine (2 × 25 mL), washed with distilled water (1 × 25 mL), and dried over $MgSO_4$. After filtration and evaporation of the solvent, the crude product was purified by column chromatography on silica gel (80:20 hexane/EtOAc). Solidification using EtOH /$CHCl_3$ gave **1** (767 mg, 0.42 mmol, 36.9%). Mp = 141−143 °C. ^{1}H NMR (499 MHz, $CDCl_3$): δ 8.32−7.07 (m, 74H, Ar−*H*), 2.72−2.70 (t, 8H, four Ar−*CH*$_2$), 1.71−1.68 (m, 8H, four Ar−CH_2−*CH*$_2$), 1.36, 1.25 (m, 24H, four (*CH*$_2$)$_3$), 0.98 (t, 12H, four terminal *CH*$_3$). ^{13}C NMR ($CDCl_3$): δ 156.2−119.4 (aromatic and vinyl carbons), 35.9, 32.0, 31.5, 29.8, 23.0, 14.5 ppm. MALDI-TOF-MS *m/z* calcd for $C_{138}H_{126}N_4$ $[M + H]^+$, 1840.0; found, 1839.8.

Synthesis of [G1−6Q] (2). Potassium *t*-butoxide (0.19 g, 1.73 mmol, 5 equiv) was dissolved in 6 mL of THF under Ar at RT. After 30 min a mixture of [G1]-CHO (1.01 g, 1.14 mmol, 3.3 equiv) and triphosphate (**18**) (0.18 g, 0.35 mmol, 1 equiv) in 15 mL of THF was added. The reaction mixture was stirred for 30 h at RT and then quenched with distilled water (1 mL), and THF was evaporated under reduced pressure. The residue was dissolved in $CHCl_3$ (30 mL). The organic layer was washed with brine (2 × 25 mL) and water (1 × 25 mL), dried ($MgSO_4$), filtered, concentrated, and purified by column chromatography on silica gel (80:20 hexane/EtOAc). Solidification using EtOH/$CHCl_3$ gave **2** (0.78 g, 0.28 mmol, 82% yield). Mp = 216−219 °C. ^{1}H NMR (499 MHz, $CDCl_3$): δ 8.24−7.01 (m, 108 H), 2.68 (t, 12H, Ar CH_2), 1.67 (t, 12H, CH_2), 1.36 (m, 36H, $(CH_2)_3$), 0.93 (t, 18H, terminal CH_3) ppm. ^{13}C NMR ($CDCl_3$): δ 156.2, 148.6, 148.2, 144.2, 138.5, 137.6, 137.5, 136.7, 129.6, 128.8, 128.8, 128.6,128.5, 128.4,128.3, 127.3, 126.2, 125.7,124.5, 124.2, 119.4, 35.8, 31,8, 31.3, 29.1, 22.7, 14.1 ppm. MALDI-TOF-MS *m/z* calcd for $C_{204}H_{186}N_6$ $[M + H]^+$, 2720.5; found, 2720.7.

Synthesis of [G2]-CHO (5). Acetyl core reagent **21** (0.22 g, 0.49 mmol, 1 equiv) and [G2]-CHO (**4**) (0.95 g, 1.0786 mmol, 2.2 equiv) were dissolved in THF (15 mL) and added dropwise to $KOC(CH_3)_3$ (0.44 g, 3.88 mmol, 3.5 equiv) in THF (5 mL). The reaction mixture was stirred for 24 h under argon atmosphere and then poured into crushed ice (30 g). $CHCl_3$ (40 mL) and 10% HCl (40 mL) were added to the cold aqueous organic mixture and vigorously stirred for 10 h at RT. The orange solution was neutralized using 10% NaOH and the aqueous layer was separated. The organic layer was washed with brine and distilled water. After the organic layer was dried over magnesium sulfate, the solvent was evaporated. The crude product was purified by column chromatography. Solidification using EtOH/$CHCl_3$ gave **5** (0.79 g, 0.42 mmol, 86.2% yield). ^{1}H NMR (499 MHz, $CDCl_3$): δ 10.09 (s, 1H, CHO), 8.24−7.17 (m, 73H, Ar−*H*), 2.71 (m, 8H, four Ar−*CH*$_2$), 1.69 (m, 8H, four *CH*$_2$), 1.35 (m, 32H, four (*CH*$_2$)$_3$), 0.93 (m, 12H, four *CH*$_3$) ppm. ^{13}C NMR ($CDCl_3$): δ 192.21 (Ar−*CHO*), 156.6, 148.8, 148.8, 148.7, 144.6, 139.8, 138.6, 137.9, 134.8, 130.6, 130.5, 129.8, 129.7, 129.1, 129.0, 128.9,128.8, 128.7, 128.5, 127.5, 127.4, 126.5, 125.9, 124.6, 119.6, 119.7, 35.9, 31.8, 31.4, 29.1, 22.7, 14.2 ppm. MALDI-TOF-MS *m/z* calcd for $C_{139}H_{126}N_4O$ $[M + H]^+$, 1868.0; found, 1867.6.

Synthesis of [G2−12Q] (3). Potassium *t*-butoxide (95%, 0.12 g, 0.98 mmol) was dissolved in 5 mL of THF under Ar at RT. After 30 min, a mixture of [G2]-CHO (**5**) (1.1 g, 0.59 mmol, 5 equiv) and triphosphate (**18**) (0.10 g, 0.20 mmol) in 15 mL of THF was added, and the reaction mixture was stirred for 16 h at RT. The reaction was then quenched with distilled water (1 mL) and THF was evaporated under reduced pressure. The residue was dissolved in $CHCl_3$ (35 mL). The organic layer was washed with water and brine, dried ($MgSO_4$), filtered, concentrated, and purified by column chromatography on silica gel (80:20 hexane/EtOAc). Solidification using EtOH/$CHCl_3$ gave **3** (773 mg, 0.13 mmol, 69.5% yield). Mp = 241−244 °C. ^{1}H NMR (499 MHz, $CDCl_3$): δ 8.35−6.80 (m, 219 H, Ar−*H*), 2.68 (t, 24H, Ar−*CH*$_2$), 1.92−1.10 (m, 96H, (*CH*$_2$)$_4$), 0.91 (t, 36H, terminal *CH*$_3$) ppm. ^{13}C NMR ($CDCl_3$): δ 156.0, 148.5, 147.8, 144,1, 138.6, 137.5, 136.5, 124.4, 130.2, 129.7, 128.5, 128.2,127.8, 127.2, 126.9, 126.0, 125.4, 124.3, 123.5, 35.7, 31.7, 29.1, 28.9, 22.7, 14.1 ppm. MALDI-TOF-MS *m/z* calcd for $C_{426}H_{384}$ N_{12} $[M + H]^+$, 5672.8; found, 5673.2.

Acknowledgment. This research was supported by the Air Force Office of Scientific Research (AFOSR) and in part by the Army Research Office. T.W.K. also thanks Kyungsung University and the Basic Research Program of the Korea Science and Engineering Foundation (KOSEF R01-2000-000-00039-0) for funding during his sabbatical leave.

Supporting Information Available: ^{1}H and ^{13}C NMR spectra of compounds **1**−**5**, **9**, **12**, and **21**, and MALDI TOF MS spectra of **1**, **2**, **4**, and **5** (pdf). These materials are available free of charge via the Internet at http://pubs.acs.org.

CM0494711